Journal of Molecular Catalysis A: Chemical 356 (2012) 14–19

Contents lists available at SciVerse ScienceDirect

Journal of Molecular Catalysis A: Chemical

journal homepage: www.elsevier.com/locate/molcata

Catalytic decomposition of nitrogen-containing heterocyclic compounds with highly dispersed iron nanoparticles on carbons

Tetsuya Matsuyama [a], Naoto Tsubouchi [b,*], Yasuo Ohtsuka [a]

[a] Institute of Multidisciplinary Research for Advanced Materials, Tohoku University, Sendai 980-8577, Japan
[b] Center for Advanced Research of Energy and Materials, Hokkaido University, Sapporo 060-8628, Japan

ARTICLE INFO

Article history:
Received 4 August 2011
Received in revised form
27 November 2011
Accepted 20 December 2011
Available online 30 December 2011

Keywords:
Pyrrole decomposition
Pyridine decomposition
Iron catalyst
N_2 formation
Hot gas cleanup

ABSTRACT

Decomposition of pyrrole or pyridine with iron catalysts supported on carbons has been studied with a cylindrical quartz-made pulse reactor, into which liquid pyrrole or pyridine is injected as a pulse, in order to develop a novel hot gas cleanup method of removing the nitrogen present in tar as N_2. The catalyst is mainly prepared by heating FeOOH precipitated onto powdery cellulose from $FeCl_3$ solution. Nanoscale iron catalysts with the average particle sizes of 25–30 nm can promote decomposition reactions of the N-containing heterocyclic compounds in inert gas at >500 °C and provide N_2 yields of 40–45% after the almost complete decomposition of pyrrole at 600 °C or pyridine at 650–700 °C. Iron catalyst with the mean size of 100–500 nm, prepared from $Fe(NO_3)_3$ impregnated with a commercial activated carbon, is also active for the decomposition of the heterocyclic N-compounds, but it is almost inactive for N_2 formation, the yields being as low as less than 2% in all cases. The increase in the number of pulses lowers the catalytic activity of iron nanoparticles for N_2 formation, whereas *in situ* H_2 treatment at 500 °C after reaction can restore it to the almost original state. On the basis of the above-mentioned results, it is likely that the activity of iron catalyst for N_2 formation from pyrrole or pyridine is very sensitive to the iron particle size, and the *in situ* H_2 treatment is effective for recovery of the decreased catalytic performance.

1. Introduction

It has been widely accepted that an integrated gasification combined cycle (IGCC) or fuel cell combined cycle (IGFC) system is one of the most environmentally acceptable technologies in order to generate electric power from organic resources, such as coal and biomass [1–3]. Dry cleanup of raw fuel gas produced in a high-temperature gasification process for IGCC or IGFC, in place of cold gas cleaning methods with wet scrubbers, has recently attracted much attention, because it can further increase the power generation efficiency of IGCC or IGFC and consequently lead to more efficient reduction of CO_2 emissions, compared with conventional pulverized coal-fired power plants [4–9]. Many studies on the high-temperature removal of impurities (e.g. H_2S and NH_3) from the raw gas have thus been carried out, and this topic has been reviewed by several workers [4,6,8,9].

The present authors' research group has been focusing on developing a hot gas cleanup method to remove low concentrations of NH_3 and tarry material in the raw gas and on utilizing inexpensive iron catalysts for this purpose [10–17], in place of Ni [6,18], Mo [6], and Ru [6]-based catalysts reported previously. We have found that nano-ordered particles of metallic iron (α-Fe), which can readily be produced by heating FeOOH precipitated on brown coals in inert gas and by H_2 reduction of FeOOH in low-valued limonite ores, achieve the almost complete decomposition of 2000 ppm NH_3 in inert gas at 750–850 °C and maintain conversion of NH_3 to N_2 at the high level of >90% at 750 °C in a fuel gas (20% CO/10% H_2/7% CO_2 or 3% H_2O balanced by He) that simulates product gas from an air-blown coal gasifier [10,13,14]. Further, it has recently been shown that FeOOH-rich limonite catalyzes the decomposition of 500–1500 ppm of tar model compounds, such as toluene and benzene, and it exhibits high benzene conversion of 95% at 700 °C in fuel gas components ($CO/H_2/CH_4/CO_2/H_2O$) produced in biomass gasification [17].

As is well-known, the nitrogen present in tar (denoted as tar-N) consists mainly of heterocyclic nitrogen structures, such as pyrrolic-N and pyridinic-N [19–23]. If these N-forms can be transformed efficiently into N_2 over iron materials, the results may contribute to the development of a novel hot gas cleanup technique of removing tar-N from the raw fuel gas. In this paper, therefore, we first examine the performances of some iron catalysts in the decomposition of pyrrole or pyridine in inert gas, and then make clear several important factors determining transformation reactions of these heterocyclic N-compounds to N_2.

* Corresponding author. Tel.: +81 11 706 6850; fax: +81 11 726 0731.
E-mail address: tsubon@eng.hokudai.ac.jp (N. Tsubouchi).

1381-1169/$ – see front matter © 2012 Elsevier B.V. All rights reserved.
doi:10.1016/j.molcata.2011.12.022

Table 1
Analyses of catalyst samples used.

Sample	Elemental analysis				Surface area[a] (m^2/g)
	C	H	N	Fe	
	(mass%-daf)			(mass%-dry)	
2% Fe/CC	95.4	0.3	–	1.8	250
7% Fe/CC	96.3	0.2	–	6.8	200
8% Fe/AC	92.2	0.5	0.4	8.3	550

[a] Measured by the BET method.

2. Experimental

2.1. Catalyst preparation

Iron catalyst was mainly loaded onto powdery cellulose (Sigma–Aldrich, Inc.) by the precipitation method using an aqueous solution of $FeCl_3$ [24]. In this method, a mixture of cellulose particles and $FeCl_3$ solution was stirred at ambient temperature, and a predetermined amount of $Ca(OH)_2$ powder was then added to precipitate the iron as FeOOH onto the cellulose. The resulting iron-loaded sample was separated from the solution by filtration, washed repeatedly with purified water to remove the remaining Ca^{2+} cations and finally carbonized with a quartz-made fixed-bed reactor in He at 800 °C to produce the iron-bearing carbon. This catalyst material is denoted as Fe/CC throughout the present paper. For a reference, $Fe(NO_3)_3$ was first impregnated with a commercial activated carbon (Nacalai Tesque, Inc.) by using the aqueous solution, and the resulting mixture after dryness was then subjected to H_2 reduction at 500 °C. The reference material obtained is denoted as Fe/AC.

Table 1 summarizes elemental analyses and surface areas of Fe/CC and Fe/AC samples with size fraction of 75–250 μm. Their iron contents on a dry basis were 1.8 mass% for 2% Fe/CC, 6.8 mass% for 7% Fe/CC, and 8.3 mass% for 8% Fe/AC, and the areas measured by the BET method after N_2 adsorption at −196 °C were in the range of 200–550 m^2/g.

2.2. Decomposition of nitrogen-containing heterocyclic compounds

Catalytic decomposition of pyrrole or pyridine was carried out under ambient pressure with a cylindrical quartz-made pulse reactor (6 mm i.d., 8 mm o.d.), which was heated with a Ni/Cr-made tape heater. The height of catalyst bed was about 3 cm, and reaction temperature was controlled by a thermocouple on the outer surface of the reactor. In a typical experiment, approximately 60 mg of the catalyst sample was first charged into the reactor and then heated in a flow of high-purity He up to 500 °C. At this temperature, the He was switched to high-purity H_2, and the catalyst sample was reduced with the H_2 for 1 h. After such a pretreatment, the reduced sample was held at a predetermined temperature (400–700 °C) in a flow of the He, and about 0.5 μl of pyrrole or pyridine was injected as a pulse into the reactor with a micro syringe to begin the reaction, the apparent contact time between gas and catalyst material being about 7 s. The effluent from the reactor exit was supplied to several gas analyses through a Pyrex (borosilicate) glass tube kept at 200 °C to prevent condensation of these N-containing heterocyclic compounds. The analytical methods are described in detail below.

2.3. Gas analysis

The amounts of N_2 and H_2 formed by the decomposition of pyrrole or pyridine were measured with a gas chromatograph (GC) equipped with a thermal conductivity detector (TCD), in which He or Ar was used as a carrier gas for the analysis of N_2 or H_2, respectively. The concentrations of the N-containing heterocyclic compounds after reaction were analyzed by the GC/flame ionization detection (FID) method. The standard analytical conditions are: column, Chromosorb-103; column temperature, 200 °C; air, 450 cm^3/min (0.5 kg/cm^2); H_2, 50 cm^3/min (0.7 kg/cm^2). Conversion of pyrrole or pyridine was estimated by using the amounts of the corresponding compound before and after reaction, whereas N_2 yield was calculated on the basis of the amounts of each form introduced and N_2 produced, and it was expressed in percent on a nitrogen basis.

2.4. Catalyst characterization

The crystalline forms of iron catalysts were examined with a powder X-ray diffraction (XRD) technique using Mn-filtered Fe-Kα radiation (30 kV, 40 mA). The average crystallite size of metallic iron (α-Fe) identified was estimated by the Debye–Scherrer method. The dispersion states of iron particles were also measured with a transmission electron microscope (TEM), the accelerating potential being 300 kV. In addition, selected catalyst samples were characterized by the Fe $2p_{3/2}$ X-ray photoelectron spectroscopy (XPS) with a non-monochromatic Mg-Kα source operating at 240 W. Binding energies of all Fe $2p_{3/2}$ spectra obtained were referred to the Ag $3d_{5/2}$ peak at 367.9 eV, according to an XPS handbook [25].

3. Results and discussion

3.1. Chemical states of iron catalysts supported on carbons

Fig. 1 presents the XRD profiles of the three catalyst samples prepared. The diffraction peaks attributable to α-Fe and iron carbide

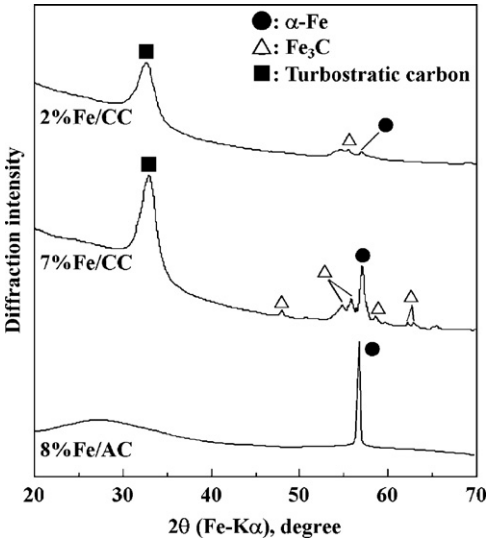

Fig. 1. XRD profiles for catalyst samples prepared.

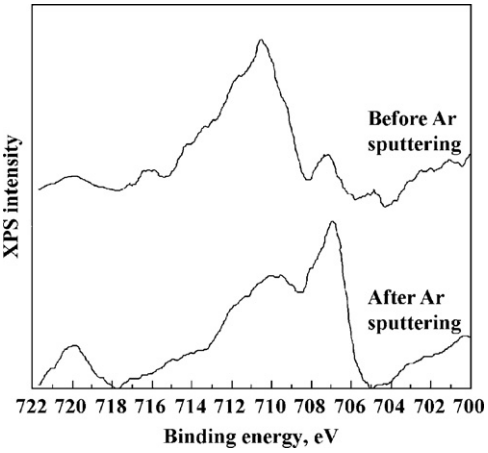

Fig. 2. Fe $2p_{3/2}$ XPS spectra before and after Ar sputtering for 7% Fe/CC.

(Fe_3C) were detectable with the 2 and 7% Fe/CC, and their signal intensities were stronger with the latter sample. The average crystallite size of α-Fe was calculated to be as small as 15 nm with the 2% Fe and 45 nm with the 7% Fe. As shown in Fig. 1, α-Fe was the only crystalline species in the 8% Fe/AC, and the crystallite size was too large (more than 100 nm) to be determined by the Debye–Scherrer method.

Fig. 1 also shows information about carbon structures due to the C(002) lines at diffraction angle (2θ) of 20–40°. The 2 and 7% Fe/CC exhibited the distinct XRD peaks attributable to turbostratic carbon at 2θ of 33.1°, whereas, with the 8% Fe/AC, any diffraction signals of the carbon could not be detected. Since it has been widely accepted that a graphite with well-organized and three-dimensional structures provides very sharp C(002) line at 2θ (Fe-Kα) of 33.6°, the turbostratic carbon is different from the graphite carbon but can be regarded as crystallized (and/or partly graphitized) carbon [26]. According to previous studies [27,28], it has also been reported that fine particles of α-Fe, which are derived from FeOOH precipitated onto low rank coals and polymers with large amounts of oxygen functional groups, catalyze crystallization and graphitization reactions of the corresponding chars and carbons produced during pyrolysis at temperatures below 1000 °C. It is thus probable that the turbostratic carbon is detectable for the Fe/CC samples prepared from oxygen-rich cellulose, whereas it is not formed significantly for the Fe/AC obtained from the activated carbon with much smaller amounts of oxygen functional groups.

Fig. 2 presents the Fe $2p_{3/2}$ XPS spectra of the 7% Fe/CC. The sample without Ar sputtering showed a small peak of α-Fe at 707.1 eV and a large, broad one of iron oxides, such as magnetite (Fe_3O_4), wustite ($Fe_{1-x}O$), and hematite (α-Fe_2O_3), around 708–714 eV. Since the oxides were observed only by the XPS method, they must be formed by oxidation of α-Fe surface upon exposure to laboratory air for sample recovery after catalyst preparation at 800 °C. No XPS signals of any iron carbides including Fe_3C identified by XRD were detectable due to partial overlapping with surface iron oxides. When this sample was exposed to Ar ion bombardment for 10 min, the surface oxides at 709–714 eV were removed, whereas the XPS intensity of α-Fe increased considerably with a corresponding increase in the intensity of the Fe $2p_{1/2}$ signal at 719.9 eV, and consequently α-Fe became the predominant form. These observations and the XRD results (Fig. 1) point out that FeOOH precipitated onto cellulose by the present method can be reduced into fine particles of α-Fe upon carbonization, and part of the α-Fe subsequently undergoes solid–solid interactions with the carbon in the CC as the Fe support to provide Fe_3C.

The TEM picture of each catalyst sample produced is shown in Fig. 3, where the size distribution of iron particles determined by the TEM is also provided. With the Fe/CC samples, iron particles with the sizes of <60 nm were finely dispersed on the CC-support (Fig. 3a and b), and the average sizes with the 2 and 7% Fe were determined to be 25 and 32 nm, respectively. The XRD results (Fig. 1) suggest that both α-Fe and Fe_3C may be included in the observed particles. As shown in Fig. 3c, the size of iron particles in the 8% Fe/AC was as large as 100–500 nm, which corresponded well to the large crystallite size (≥100 nm) of α-Fe identified by XRD. It has been accepted that the iron precipitated onto oxygen-rich low rank coals from $FeCl_3$ solution is present as fine particles of FeOOH with the size of <5 nm, which can lead to the formation of highly dispersed iron particles upon pyrolysis [29]. On the other hand, $Fe(NO_3)_3$ impregnated with the activated carbon poor in oxygen component resulted in low dispersion of iron particles. It is thus probable that the formation of smaller nanoparticles observed with the Fe/CC samples prepared from oxygen-rich cellulose is attributed to higher dispersion of the precipitated iron.

3.2. Decomposition of pyrrole and formation of N_2

Fig. 4a shows the temperature dependency of pyrrole conversion over the 7% Fe/CC. In a blank experiment with the CC-support alone, the decomposition of pyrrole took place above 400 °C, and the conversion at 600 °C was approximately 75%. Since it has been reported that thermal decomposition of pyrrole takes place predominantly at the temperature range of 750–850 °C [30], the carbon in the CC may promote the decomposition reaction. As seen in Fig. 4a, the catalytic effect of the Fe on the reaction appeared apparently at about 500 °C, and the conversion tended to increase more remarkably with increasing temperature than without the Fe and reached almost 100% at 600 °C.

The influence of the number of pulses on the conversion at 600 °C is summarized in Table 2, where the mean value of the two experiments is provided. With the CC-support alone, the conversion decreased considerably with increasing pulse number, and the value at six pulses was less than 45%. Such a decrease might be caused by the deposition of pyrrole-derived carbon on active C-atoms for the decomposition of pyrrole. On the other hand, the 7% Fe/CC exhibited very stable catalytic performance under the conditions applied, and the conversion was almost unchanged to be more than 99% (Table 2).

Fig. 4b illustrates N_2 yield in each experiment shown in Fig. 4a. No appreciable amount of N_2 was detectable with the CC-support alone, irrespective of reaction temperature, which means that the support has almost no effect on N_2 formation from pyrrole under the present conditions. As shown in Fig. 4b, the 7% Fe/CC was almost inactive at the temperature range of 400–500 °C, but it promoted the formation reaction after 500 °C, and the catalytic activity

Table 2
Influence of the number of pulses on pyrrole conversion and N_2 yield at 600 °C.

Sample	Number of pulses	Pyrrole conversion[a] (mol%)	N_2 yield[a] (N-%)
CC	1	74	Nil[b]
	2	71	Nil[b]
	4	59	Nil[b]
	6	43	Nil[b]
7% Fe/CC	1	>99	41
	2	>99	41
	4	>99	35
	6	>99	26
8% Fe/AC	1	97	2
	2	97	2

[a] Average value of the repeated experiments.
[b] Less than 0.1 N-%.

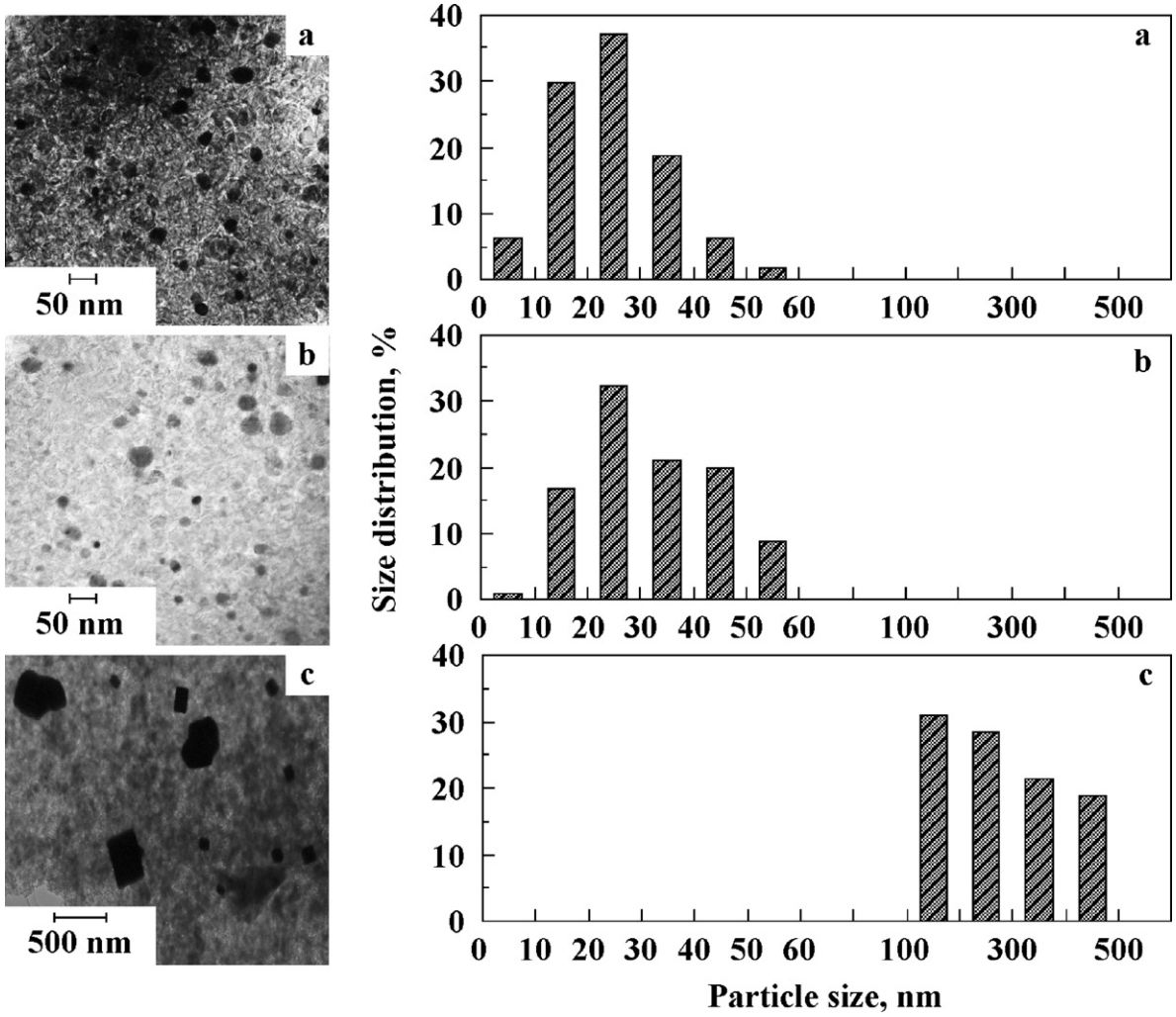

Fig. 3. TEM pictures of catalyst samples produced and size distribution of iron particles determined by TEM: (a) 2% Fe/CC, (b) 7% Fe/CC, and (c) 8% Fe/AC.

increased considerably with increasing temperature. The yield was estimated to be almost 0% at 500 °C, 2–3% at 550 °C, and about 40% at 600 °C.

Table 2 also shows the influence of the number of pulses on the yield at 600 °C. As can be expected from the results given in Fig. 4b, the yield with the CC-support alone was always negligibly low (<0.1%). On the other hand, the 7% Fe/CC could catalyze N_2 formation in all cases, but the catalytic effect tended to decrease with increasing pulse number, the yield at six pulses being approximately 25%. Such a catalyst deactivation may be caused by agglomeration of iron nanoparticles and/or by the formation of iron carbides by the reaction of α-Fe with the carbon in the Fe/CC or pyrrole-derived carbon.

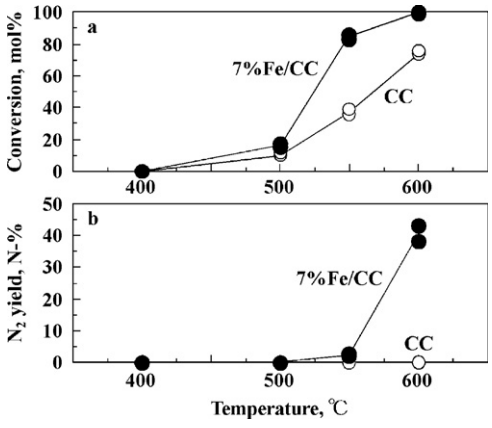

Fig. 4. Effect of temperature on pyrrole conversion (a) and N_2 yield (b) over CC without Fe and 7% Fe/CC.

When the 8% Fe/AC was used in place of the 7% Fe/CC, pyrrole conversions exceeded 95%, but N_2 yields were only 2% (Table 2), which was much lower than the values (26–41%) with the Fe/CC. Since the TEM analyses revealed that the size of iron particles in the Fe/AC was as large as 100–500 nm (Fig. 3c), compared with that (<60 nm) of the Fe/CC, it is probable that the more finely dispersed iron works more efficiently as the catalyst for N_2 formation from pyrrole.

3.3. Decomposition of pyridine and formation of N_2

Fig. 5a is the temperature dependency of pyridine conversion over the 2 and 7% Fe/CC. With the CC-support alone, the conversion was almost 0% at 400 °C, but it increased with increasing temperature to be >80% at 700 °C. The carbon in the CC may promote the decomposition of pyridine as well as pyrrole (Fig. 4a), because it has been reported that thermal decomposition of pyridine occurs predominantly at high-temperatures above 800 °C [30]. The 2 and 7% Fe/CC were both effective for decomposing pyridine, and the effectiveness was slightly larger with the latter sample (Fig. 5a).

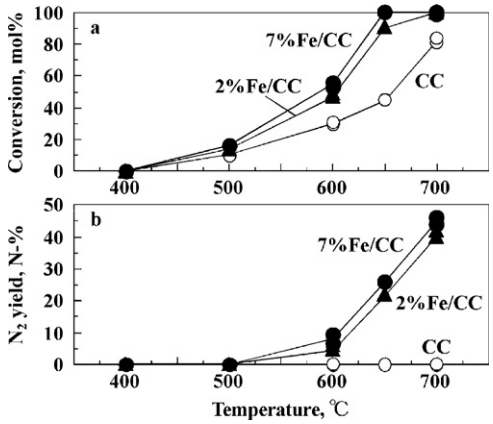

Fig. 5. Effect of temperature on pyridine conversion (a) and N_2 yield (b) over CC without Fe, 2 and 7% Fe/CC.

The conversion was larger at a higher temperature, regardless of iron loading, and the almost complete decomposition of more than 99% occurred apparently at 650 °C with the 7% Fe and at 700 °C with the 2% Fe.

Table 3 illustrates the influence of the number of pulses on the conversion at 700 °C. The conversion with the CC-support alone decreased considerably after two pulses, and the value at eight pulses was about 35%. Such a trend was almost similar to that (Table 2) of the pyrrole conversion observed with the corresponding sample. It is possible that carbon to be formed from pyridine as well as pyrrole might lower the reactivity of active C-atoms in the CC. As shown in Table 3, the 2% Fe/CC maintained very high pyridine conversion of more than 99% up to four pulses and then exhibited the decrease in the activity, whereas, with the 7% Fe/CC, there was no activity decay, and the conversion was almost unchanged to be >99%.

Fig. 5b presents N_2 yield in each run shown in Fig. 5a. With the CC-support alone, the yields were negligibly small at all of the temperatures. This result means that the support is almost ineffective for N_2 formation from pyridine as well as pyrrole (Fig. 4b). In contrast to the uncatalyzed pyridine decomposition, the yields with the 2 and 7% Fe/CC increased considerably beyond 600 °C, and the values at 650 and 700 °C ranged 20–25% and 40–45%, respectively.

Table 3
Influence of the number of pulses on pyridine conversion and N_2 yield at 700 °C.

Sample	Number of pulses	Pyridine conversion[a] (mol%)	N_2 yield[a] (N-%)
CC	1	83	Nil[b]
	2	81	Nil[b]
	4	70	Nil[b]
	6	54	Nil[b]
	8	36	Nil[b]
2% Fe/CC	1	>99	42
	2	>99	37
	4	>99	29
	6	97	19
	8	91	5
7% Fe/CC	1	>99	45
	2	>99	44
	4	>99	39
	6	>99	33
	8	>99	26
Used 7% Fe/CC	1	>99	44
8% Fe/AC	1	97	2
	2	95	1

[a] Average value of the repeated experiments.
[b] Less than 0.1 N-%.

Table 4
Yields of N_2 and H_2 formed during CH_3CN decomposition at 600 °C with 7% Fe/CC or 8% Fe/AC.

Sample	Number of pulses	N_2 yield (N-%)	H_2 yield (H-%)
7% Fe/CC	1	20	23
8% Fe/AC	1	2	2

Table 3 also summarizes the influence of the number of pulses on the yield at 700 °C. As can be expected from Fig. 5b, no measurable amounts of N_2 were detectable with the CC-support alone in any cases. On the other hand, the 2 and 7% Fe/CC could promote N_2 formation in every case, but their catalytic activity decreased considerably with increasing pulse number. The extent of the decrease was larger with the former sample, and the yield at eight pulses was 5 or 26% with the 2 or 7% Fe, respectively (Table 3). When the used 7% Fe/CC was subjected first to *in situ* H_2 treatment at 500 °C for 1 h and then to the decomposition run of pyridine at 700 °C, the yield was restored to the initial level of about 45% (Table 3). The deactivation of the 2–7% Fe catalysts observed in Table 3 may thus be caused by the deposition of pyridine-derived carbon on active iron sites for N_2 formation, and the *in situ* H_2 treatment may be effective for recovery of the decreased catalytic activity.

The results for pyridine conversion and N_2 yield over the 8% Fe/AC are also shown in Table 3. The Fe/AC was effective for the decomposition of pyridine, and the conversions were as large as 95–97% under the conditions applied. When the yields with the Fe/AC and the 2–7% Fe/CC were compared at the high conversions above 95%, the value of the former (Table 3) was significantly lower with the Fe/AC with large iron particles of 100–500 nm (Fig. 3). These observations mean that the activity of iron catalyst for N_2 formation from pyridine depends strongly on the dispersion of iron particles.

3.4. Speculated mechanisms for iron-catalyzed formation of N_2 from pyrrole and pyridine

As mentioned above, the decomposition of these N-containing heterocyclic compounds occurred at the temperature range of 500–700 °C, regardless of the absence or presence of iron catalysts, and the degree was always higher in the latter case under the conditions applied (Figs. 4a and 5a and Tables 2 and 3). In addition, N_2 formation from the heterocyclic N-compounds proceeded dominantly in the presence of nanoscale iron particles (Figs. 4b and 5b and Tables 2 and 3). Further, it has been reported that most of the nitrogen present in pyrrole or pyridine is thermally decomposed into cyanide forms (for example, hydrogen cyanide (HCN), ethynyl cyanide (HCCCN), and methyl cyanide (CH_3CN)) at ≥750 or 800 °C, respectively [31–34]. On the basis of this information and the above-described results, the iron and carbon in the Fe/CC and Fe/AC samples may promote the transformation of the heterocyclic N-compounds to cyanide species, which might subsequently be decomposed over iron nanoparticles to provide N_2.

To discuss the possibility of the latter reaction, about 0.5 μl of CH_3CN was passed over the 7% Fe/CC or the 8% Fe/AC at 600 °C, and yields of both N_2 and H_2 formed were investigated. The results are shown in Table 4. Significant amounts of N_2 and H_2 were detectable with the Fe/CC, and yields of these species were determined to be both approximately 20%, indicating molar N_2/H_2 ratio of nearly 1/3. According to this result, it may be reasonable to suppose that overall reaction for the formation of N_2 and H_2 in the present CH_3CN decomposition is expressed as Eq. (1).

$$CH_3CN \rightarrow 0.5\,N_2 + 1.5H_2 + 2C \quad (1)$$

When the Fe/AC with large iron particles of 100–500 nm (Fig. 3) was used in place of the Fe/CC, as shown in Table 4, yields of N_2 and

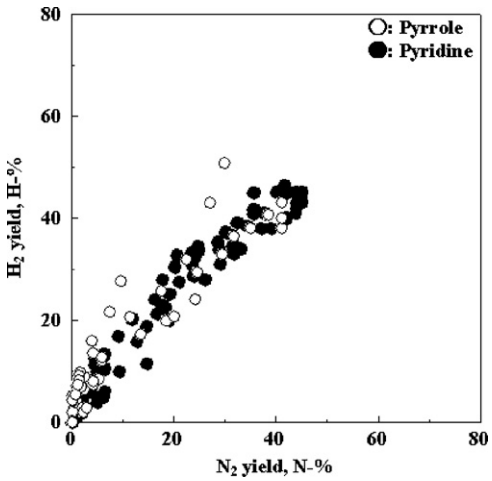

Fig. 6. Relationship between yields of N_2 and H_2 formed in each experiment shown in Figs. 4 and 5 and Tables 2 and 3.

H_2 decreased to about one-tenth of those with the latter sample. It is thus evident that the activity of iron catalyst for the formation of N_2 and H_2 from CH_3CN is very sensitive to the iron particle size.

It is of interest to compare yields of N_2 and H_2 formed in each experiment given in Figs. 4 and 5 and Tables 2 and 3. The results are illustrated in Fig. 6. Although some data were scattered, there was an almost 1:1 linear correlation between both yields. On the basis of this result and the above-mentioned discussion, it is possible that HCN, HCCCN, and CH_3CN derived from pyrrole or pyridine over the present catalyst samples, if they are actually produced, may subsequently be decomposed into N_2 and H_2 by the catalysis of nano-ordered iron particles detected by the TEM (Fig. 3), and overall reactions for the iron-catalyzed decomposition of these cyanides may be expressed as Eqs. (1)–(3), respectively.

$$HCN \rightarrow 0.5\,N_2 + 0.5H_2 + C \quad (2)$$

$$HCCCN \rightarrow 0.5\,N_2 + 0.5H_2 + 3C \quad (3)$$

Because the formation of N_2 and H_2 from CH_3CN was much higher with the Fe/CC than with the Fe/AC (Table 4), the highly dispersed iron particles on the CC-support may also work more efficiently for decomposing HCN and HCCCN. To clarify the mechanism of iron-catalyzed formation of N_2 from pyrrole or pyridine in detail and investigate the catalytic performance of the Fe/CC in a fuel gas from coal or biomass should be the subject of future work.

4. Conclusions

In order to develop a novel hot gas cleanup method of removing the nitrogen present in tar as N_2, the performances of iron catalysts in the decomposition of pyrrole or pyridine have been studied with a cylindrical quartz-made pulse reactor, into which liquid pyrrole or pyridine is injected as a pulse. When 2–8 mass% Fe catalysts are prepared from FeOOH precipitated onto powdery cellulose and from $Fe(NO_3)_3$ impregnated with a commercial activated carbon, designated as Fe/CC and Fe/AC, they promote the decomposition of the N-containing heterocyclic compounds in inert gas at 500–700 °C, and 2–7% Fe/CC can give N_2 yields of 40–45% after the almost complete decomposition of pyrrole at 600 °C or pyridine at 650–700 °C, whereas 8% Fe/AC has almost no effect on N_2 formation in any cases. The TEM observations point out that nanoscale iron particles with the sizes of 25–30 nm can catalyze the formation reaction efficiently. Although the increase in the number of pulses decreases the catalytic activity of iron nanoparticles for N_2 formation, *in situ* H_2 treatment of the used Fe/CC at 500 °C restores it to the almost original state. Since H_2 is one of the main components in fuel gas produced from coal or biomass, the above-described results suggest that the highly dispersed iron catalysts might work more efficiently for N_2 formation from pyrrole or pyridine in the hot fuel gas, though the catalytic activity should be investigated in the future work.

Acknowledgement

This work was supported in part by a Grant-in-Aid for Scientific Research from the Ministry of Education, Science, Sports and Culture, Japan (No. 05558072).

References

[1] S. Benson, Fuel Cells – Use with Coal and Other Solid Fuels, IEA Coal Research, London, UK, 2001, CCC/47.
[2] C. Henderson, Clean Coal Technologies, IEA Coal Research, London, UK, 2003, CCC/74.
[3] S.J. Mills, Coal Gasification and IGCC in Europe, IEA Coal Research, London, UK, 2006, CCC/113.
[4] K.V. Thambimuthu, Gas Cleaning for Advanced Coal-Based Power Generation, IEA Coal Research, London, UK, 1993, IEACR/53.
[5] E. Schmidt, P. Gäng, T. Pilz, A. Dittler (Eds.), High Temperature Gas Cleaning, G. Braun Printconsult GmbH, Karlsruhe, Germany, 1996.
[6] S.C. Mitchell, Hot Gas Cleanup of Sulfur, Nitrogen, Minor and Trace Elements, IEA Coal Research, London, UK, 1998, CCC/12.
[7] A. Dittler, G. Hemmer, G. Kasper (Eds.), High Temperature Gas Cleaning, vol. II, G. Braun ems GmbH, Karlsruhe, Germany, 1999.
[8] Y. Ohtsuka, N. Tsubouchi, T. Kikuchi, H. Hashimoto, Powder Technol. 190 (2009) 340–347.
[9] C. Xu, J. Donald, E. Byambajav, Y. Ohtsuka, Fuel 89 (2010) 1784–1795.
[10] Y. Ohtsuka, C. Xu, D. Kong, N. Tsubouchi, Fuel 83 (2004) 685–692.
[11] C. Xu, N. Tsubouchi, H. Hashimoto, Y. Ohtsuka, Fuel 84 (2005) 1957–1967.
[12] N. Tsubouchi, H. Hashimoto, Y. Ohtsuka, Catal. Lett. 105 (2005) 203–208.
[13] N. Tsubouchi, H. Hashimoto, Y. Ohtsuka, in: C. Kanaoka, H. Makino, H. Kamiya (Eds.), Advanced Gas Cleaning Technology, Jugei Shobo, Tokyo, Japan, 2005, pp. 483–487.
[14] N. Tsubouchi, H. Hashimoto, Y. Ohtsuka, Energy Fuels 21 (2007) 3063–3069.
[15] N. Tsubouchi, H. Hashimoto, Y. Ohtsuka, Powder Technol. 180 (2008) 184–189.
[16] J. Donald, C. Xu, H. Hashimoto, E. Byambajav, Y. Ohtsuka, Appl. Catal. A Gen. 375 (2010) 124–133.
[17] Y. Ohtsuka, J. Donald, E. Byambajav, H. Hashimoto, T. Kikuchi, C. Xu, Proceedings of the 10th Japan–China Symposium on Coal and C_1 Chemistry (CD-ROM), Tsukuba, Japan, July 26–29, 2009.
[18] D. Świerczyński, S. Libs, C. Courson, A. Kiennemann, Appl. Catal. B Environ. 74 (2007) 211–222.
[19] P.R. Solomon, M.B. Colket, Fuel 57 (1978) 749–755.
[20] M.J. Wornat, A.F. Sarofim, J.P. Longwell, A.L. Lafleur, Energy Fuels 2 (1988) 775–782.
[21] P.F. Nelson, M.D. Kelly, M.J. Wornat, Fuel 70 (1991) 403–407.
[22] J. Leppälahti, T. Koljonen, Fuel Process. Technol. 43 (1995) 1–45.
[23] H. Zhang, T.H. Fletcher, Energy Fuels 15 (2001) 1512–1522.
[24] K. Asami, Y. Ohtsuka, Ind. Eng. Chem. Res. 32 (1993) 1631–1636.
[25] J.F. Moulder, W.F. Stichle, P.E. Sobol, K.D. Bomben (Eds.), Handbook of X-ray Photoelectron Spectroscopy, Perkin-Elmer, Eden Praine, USA, 1992.
[26] A. Oya, S. Otani, Carbon 19 (1981) 391–400.
[27] Y. Ohtsuka, T. Watanabe, K. Asami, H. Mori, Energy Fuels 12 (1998) 1356–1362.
[28] Y. Ohshima, N. Tsubouchi, Y. Ohtsuka, Appl. Catal. B Environ. 111–112 (2012) 614–620.
[29] Y. Ohtsuka, K. Asami, Catal. Today 39 (1997) 111–125.
[30] O.S.L. Bruinsma, P.J.J. Tromp, H.J.J. de Sauvage Nolting, J.A. Moulijn, Fuel 67 (1988) 334–340.
[31] A. Lifshitz, C. Tamburu, A. Suslensky, J. Phys. Chem. 93 (1989) 5802–5808.
[32] C.D. Hurd, J.I. Simon, J. Am. Chem. Soc. 84 (1962) 4519–4524.
[33] A.E. Axworthy, V.H. Dayan, G.B. Martin, Fuel 57 (1978) 29–35.
[34] T.J. Houser, M.E. McCarville, T. Biftu, Int. J. Chem. Kinet. 12 (1980) 555–568.